

Article

Cutting Energy Consumption Modelling of End Milling Cutter Coated with AlTiCrN

Yue Meng¹, Xinsheng Sun¹, Shengming Dong¹, Yue Wang² and Xianli Liu^{1,*}

¹ Key Laboratory of Advanced Manufacturing and Intelligent Technology, Ministry of Education, Harbin University of Science and Technology, Harbin 150080, China; mengyue5250@163.com (Y.M.)

² Cummin Inc., 500 Jackson Street, Columbus, IN 47201, USA

* Correspondence: xliu@hrbust.edu.cn; Tel.: +86-139-4511-1601

Abstract: As an indispensable piece of equipment in the manufacturing industry, the machine tool is low-energy-efficiency and high-energy-consumption in operation. Therefore, it is urgent to establish a cutting energy consumption model to guide production and reduce the energy consumption of the machining process. In this paper, the AlTiCrN-coated cutting tool is taken as the object of study, and the cutting energy consumption model is established. The cutting energy consumption model is composed of a machining time model and a cutting power model. The cutting power model can be divided into the shear deformation power model of the workpiece, the friction power model of the flank surface and the friction power model of the rake surface. The influence of the edge shape is taken into account in the establishment of the friction power model of the flank surface. The machining time model considering the S-type acceleration and deceleration stage is established. The accuracy of the model was verified by experiments. Experimental results show that the model has high accuracy. The Taguchi method was used to carry out the numerical experiment with the cutting energy consumption of the machine tool as the response. The influences of cutting parameters on energy consumption are analyzed. Cutting width is the most important factor, followed by cutting depth, then feed rate and spindle speed. The physical principle of the influence of cutting parameters on cutting energy consumption is revealed.

Keywords: cutting energy consumption; coated cutting tool; cutting parameter; modelling; machining time



Citation: Meng, Y.; Sun, X.; Dong, S.; Wang, Y.; Liu, X. Cutting Energy Consumption Modelling of End Milling Cutter Coated with AlTiCrN. *Coatings* **2023**, *13*, 679. <https://doi.org/10.3390/coatings13040679>

Academic Editor: Ivan A. Pelevin

Received: 28 February 2023

Revised: 16 March 2023

Accepted: 20 March 2023

Published: 27 March 2023



Copyright: © 2023 by the authors. Licensee MDPI, Basel, Switzerland. This article is an open access article distributed under the terms and conditions of the Creative Commons Attribution (CC BY) license (<https://creativecommons.org/licenses/by/4.0/>).

1. Introduction

With the development of society, people's demand for energy is increasing. The large consumption of fossil energy led to a series of environmental problems and an energy crisis. As one of the largest energy consumption industries, the manufacturing industry is an important source of energy consumption and environmental pollution. The machine tool is widely used in machining, and the problems of high processing energy consumption and low energy efficiency have always existed. As shown in Figure 1, this is an example of the machine tool power. Cutting power is an important part in the total power of the machine tool. Newman et al. [1] points out that the energy used to remove the material is less than 25% of the total energy consumption in the actual cutting process. Machine tools cost a lot of energy in manufacturing [2]. Energy efficiency is an important indicator of performance in manufacturing. Therefore, it is urgent to study the cutting process energy consumption of the machine tool to guide production and reduce energy waste.

Gutowski et al. [3] propose the concept of fixed energy and cutting energy by studying the energy consumption of machine tools. Zhou et al. [4] believe that the change of energy consumption in end milling is mainly achieved by changing the average chip thickness. Balogun et al. [5] study the influence of undeformed chip thickness, tool wear, dry and flood coolant, and cutting tool nose radius on the cutting energy consumption of machine tools. Rodriguez-Alabanda et al. [6] study the influence of different machining strategies

and cutting parameters on the energy consumption of the machine tool in roughing and finishing of an EN-AW 7075 mold. Rodrigues et al. [7] experimentally study the influence of tool chip breaker chamfer angle on specific cutting energy under conventional cutting speed and high-speed cutting. Liu et al. [8] find that tool wear has small effect on the specific energy at the machine tool and spindle level. At the processing level, the degree of tool wear has a significant effect on the net specific cutting energy. The above researchers study the influence of various parameters on energy consumption from different perspectives and provide new ideas for the study of energy consumption.

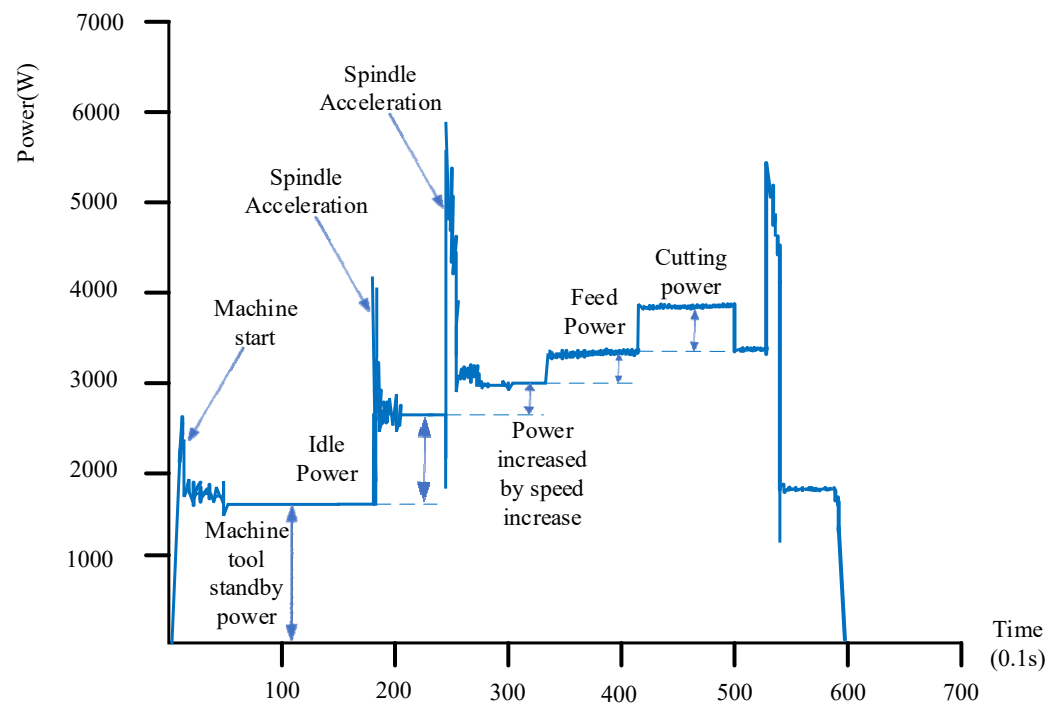


Figure 1. Machine power diagram.

Liu et al. [9] and Zhang et al. [10] consider the size effect of specific cutting force, feed per tooth, axial cutting depth, and radial cutting width in the power model. Nur et al. [11] propose the using of measured cutting forces to calculate the electrical energy consumption during the finish turning process of metals. Refs. [12–14] establish a cutting power model which considers tool wear from the perspective of cutting force. The tool wear in the model of Hu et al. [12] and Li et al. [13] are linear function. the tool wear in the model of Shi et al. [14] are quadratic function. Jiang et al. [15] establish an instantaneous energy consumption model considering milling vibration and tool tooth error based on milling force. The energy consumption models are established by the cutting force in the above literature. Although it can well reveal the principle of cutting energy consumption, the established model ignores the influence of chips on cutting energy consumption in the cutting process.

Awan et al. [16] compares the accuracy of three supervised learning techniques, Gaussian process regression, regression tree and artificial neural network, in predicting machine tool energy consumption, and find that the Gaussian process regression has the smallest error in the verification and testing process. Brillinger et al. [17] study the prediction ability of Decision Tree, Random Forest and Boosted Random Forest for machine tool energy consumption. Among the three algorithms, Random Forest has the highest prediction accuracy. Machine learning is widely used to predict the energy consumption of machine tool in recent years. Although the prediction accuracy is high, it cannot explain the impact trends and principles of cutting parameters on energy consumption.

Pawanr et al. [18] establish an empirical model between material removal rate and energy consumption in the turning process by the response surface method. Based on the study of energy consumption in the milling process of AISI 304 stainless steel, Yu et al. [19] establish an empirical model of specific energy consumption of machine tools considering tool wear and workpiece surface hardness. Pawanr et al. [20] establish an empirical model to predict the transient energy consumption of machine tools. Zhao et al. [21] develop an empirical model of specific cutting energy considering tool wear. In the above literature, the empirical models of machine tool energy consumption are established from the experimental point of view. Although these models can express the impact trend of cutting parameters on energy consumption, they cannot explain how cutting parameters affect energy consumption in principle. The prediction accuracy is lower than that of machine learning methods.

Ma et al. [22] evaluate the cutting energy consumption and energy efficiency of 4140 steel based on the numerical analysis of the AdvantEdge finite element method. Abele et al. [23] propose a simulation method combining model-based cutting process simulation and machine tool component simulation. The model is used to monitor and predict the energy consumption of machine tools. Pawar et al. [24] propose a hybrid model of milling power for variable curved geometry. The prediction method of cutting energy consumption provided in the above literature has the problems of poor universality and complicated application.

In summary, most of the current research on machine tool energy consumption is aimed at the overall level of the machine tool. Only a small part of the research focuses on the study of cutting energy consumption. The existing cutting energy consumption models doesn't consider the influence of chips produced in the cutting process on cutting energy consumption. Most of the models established in the above literature are based on cutting power. Only the influence of cutting power on cutting energy consumption is considered. However, the machining time is an important factor affecting cutting energy consumption. Moreover, the change of feed rate at the corner needs to be considered, and it is necessary to establish a machining time model to predict the cutting energy consumption. The tool edge shape is also an important factor affecting cutting energy consumption. In this paper, a general cutting energy consumption model is established from the perspective of chip formation.

The rest of the structure is as follows. The second part introduces the modelling method of cutting energy consumption. A cutting energy consumption model considering the shape of the tool edge and the acceleration and deceleration of the feed rate at the corner is proposed. The cutting power model is improved by analyzing the influence of the geometric shape of the tool edge on friction energy. The S-type acceleration and deceleration process at the corner is modeled and calculated, and the machining time model is improved. In the third part, the accuracy of the cutting energy consumption model is verified by experiments, and the influence of cutting depth and cutting width on cutting energy consumption is analyzed. In the fourth part, the influence of cutting parameters on the cutting energy consumption of a machine tool are analyzed theoretically and verified by the Taguchi experiment. The influence mode and primary and secondary relationship of cutting parameters on cutting energy consumption are obtained. The selection of cutting parameters is discussed. The optimal combination of machining parameters in the experimental range is $n = 3000$, $v_f = 300$, $a_p = 2$ and $a_e = 0.3$. The last part summarizes the full paper. The structure of this paper is shown in Figure 2.

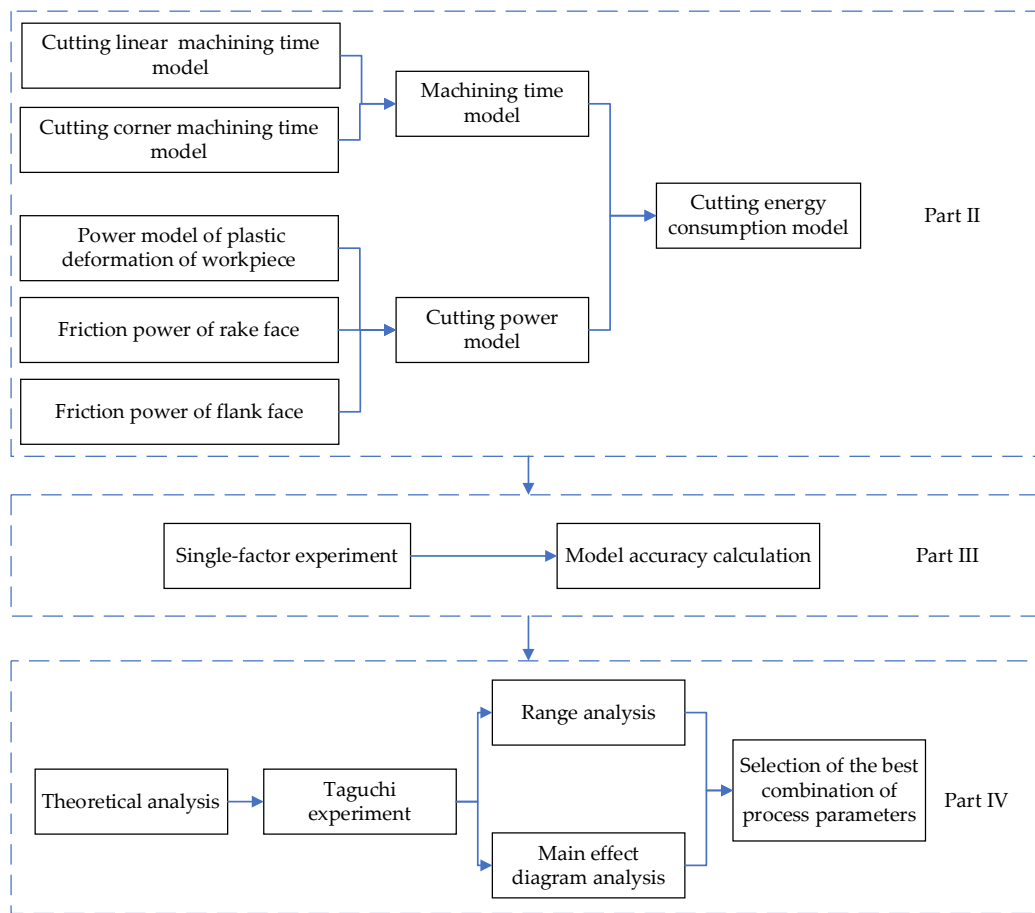


Figure 2. Paper structure.

2. Modelling of Cutting Energy Consumption

Energy consumption is the integration of power in time, which can be expressed as

$$E = \int_{t_1}^{t_2} P_t dt \quad (1)$$

where P_t is the instantaneous power, and E is the energy consumption of time t_1 to t_2 . Therefore, the cutting energy consumption is analyzed from the two factors of cutting power and machining time.

2.1. Cutting Power Model of Machine Tool

The metal deformation process of the cutting layer is roughly divided into three deformation zones, as shown in Figure 3. The first deformation zone is the main deformation zone. As the cutting tool approaches, the metal generates shear deformation along the slip line. The power consumed at this stage is the plastic deformation power P_p . In the second deformation zone, the chip is further squeezed by the rake face when it is discharged along the rake face, resulting in friction. The power consumed in this stage is the friction power P_{fr} of the rake face. In the third deformation zone, the machined surface is subjected to the extrusion, friction, and spring back of the cutting edge and the flank face. The power consumed in this stage is the friction power of the flank face P_{ff} . Other energies involved in the cutting process are chip kinetic energy, surface energy, and elastic deformation energy P_e .

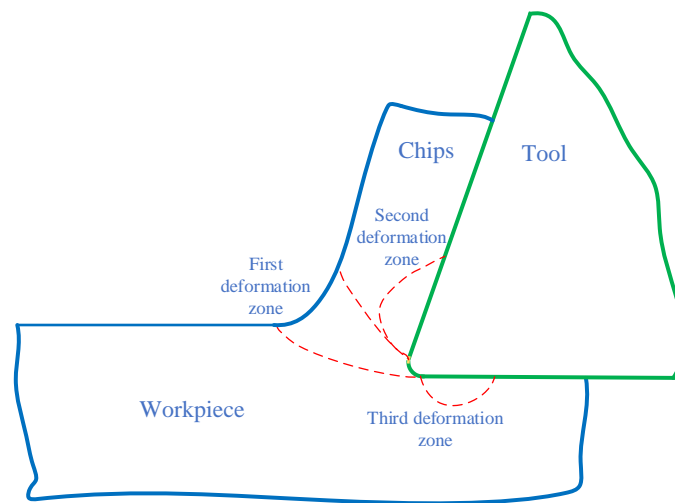


Figure 3. Three deformation zones in metal cutting.

Therefore, the cutting power is established by the following three parts:

The first part is the plastic deformation power P_p . The second part is the friction power consumed at contact zone of cutting tool and workpiece P_f , which including friction power consumed at rake face in second deformation zone P_{fr} and friction power consumed at flank face in third deformation zone P_{ff} . The third part is kinetic energy of chip, surface energy of workpiece, and elastic deformation power P_e .

The sum of the above-consumed power is equal to the cutting power of the machine tool. Therefore, the cutting power P_c is expressed by Equation (2).

$$P_c = P_p + P_f + P_e \quad (2)$$

Experiments results show that the power caused by chip kinetic energy, surface energy, and elastic deformation energy can be neglected in cutting [25].

2.2. Power Model of Plastic Deformation of Workpiece

In the first deformation zone, the work done by the stress σ_{ij} on the corresponding deformation $d\varepsilon_{ij}$, is equal to the strain energy of the object. Assuming that the plastic deformation volume is constant, the plastic deformation work is the work of the shape change of the deformed body. If the volume of the unit is V , the plastic deformation work consumed by the unit during plastic deformation is expressed by Equation (3).

$$dW_p = dU = \iiint_V \sigma_{ij} d\varepsilon_{ij} dV \quad (3)$$

The equivalent stress is expressed by $\sigma_i = \sqrt{3}K \cdot (\ln \zeta)^n$, Von Mises equivalent strain is expressed by $\varepsilon_i = \frac{2\sqrt{3}}{3} \ln \zeta$. the ideal material removal volume is expressed by $V = L_{total} \cdot a_p \cdot a_e = a_p \cdot a_e \cdot v_f \cdot t_{pro}$, where, a_p is the cutting depth, a_e is the cutting width, v_f is the feed rate, t_{pro} is the cutting time. Substituting Equation (2), the plastic deformation power consumed in the cutting process P_p can be expressed as

$$P_p = 2K \left(\ln \frac{\cos(\varphi - \gamma_0)}{\sin \varphi} \right)^{n_0+1} a_p a_e v_f \quad (4)$$

2.3. Friction Power Model of Rake Face

Assuming that the chip leaves after passing the length l_c on the rake face, the average friction stress on the rake face is set to $\bar{\tau}_c$. Therefore, the friction force consumed on the

rake face tool-chip contact surface is $\bar{\tau}_c A$. The friction work per unit time can be expressed by Equation (5).

$$P_{fr} = \bar{\tau}_c A v_{chip} \quad (5)$$

where A is the contact zone, and v_{chip} is the velocity of the chip flowing out along the rake face of the tool, which can be expressed by Equation (6).

$$v_{chip} = \frac{\sin \varphi}{\cos(\varphi - \gamma)} v \quad (6)$$

where v is the cutting speed, expressed by $v = \pi dn/1000$, n is the spindle speed, d is the cutting tool diameter, φ is the shear angle, and γ is the rake angle.

The average friction stress on the rake face is $\bar{\tau}_c = k_c \tau_c$, where τ_c is the shear deformation stress of the processed material. k_c is the ratio of the actual contact zone to the apparent contact zone, which is generally 0.8.

The contact zone $A = bl_{fr}$, where b is the cutting width, and l_{fr} is the theoretical cutting tool-chip contact length. The relationship between the theoretical contact length and the actual contact length l_c can be expressed by Equation (7).

$$l_c = k_m l_{fr} = k_m \frac{h \sin(\varphi + \beta - \gamma)}{\sin \varphi \cos \beta} \quad (7)$$

where k_m is the ratio of the actual contact length to the theoretical contact length, which is generally 2.0, and h is the thickness of the workpiece to be cut.

According to Equations (5)–(7), the friction work on the rake face is obtained.

$$P_{fr} = \frac{\pi k_c k_m \sin(\varphi + \beta - \gamma)}{1000 \cos \beta \cos(\varphi - \gamma)} \tau_c d n b h \quad (8)$$

2.4. Friction Power Model of Flank Face

The contact length between the flank face and the machined surface is l_{ff} , and the average friction stress of the contact zone is τ_{cf} . Then the friction force acting on the contact zone is $\tau_{cf} l_{ff} b$, and the friction work consumed per unit time can be expressed by Equation (9).

$$P_{ff} = \tau_{cf} b l_{ff} v \quad (9)$$

In this study, the AlTiCrN coated tool is a new cutting tool, the cutting tool edge has not been worn, and the cutting tool edge is a sharp cutting edge.

As shown in Figure 4, when cutting edge is sharp, the contact length between the flank face and the machined surface is expressed by $l_{ff} = h_{re} \cot \alpha$. The consumed friction power can be expressed by Equation (10).

$$P_{ffa} = \tau_{cf} b v h_{re} \cot \alpha \quad (10)$$

where α is the tool clearance.

The cutting width b is regarded as a_e , and the workpiece thickness h is regarded as a_p . Therefore, the cutting power with the sharp cutting edge can be calculated by Equation (11).

$$P_c = P_p + (P_{fr} + P_{ff}) = K_1 a_p a_e v_f + (K_2 n a_e a_p + K_3 n a_e) \quad (11)$$

where

$$K_1 = 2K \left(\ln \frac{\cos(\varphi - \gamma_0)}{\sin \varphi} \right)^{n_0+1}, K_2 = \frac{\pi \tau_c d k_c k_m \sin(\varphi + \beta - \gamma)}{1000 \cos \beta \cos(\varphi - \gamma)}, K_3 = \frac{\pi d \tau_{cf} h_{re} \cot \alpha}{1000}$$

The model established in this paper is used for the general cutting of plastic materials. Before applying this model, the finite element method can be adopted to simulate the metal properties [26,27].

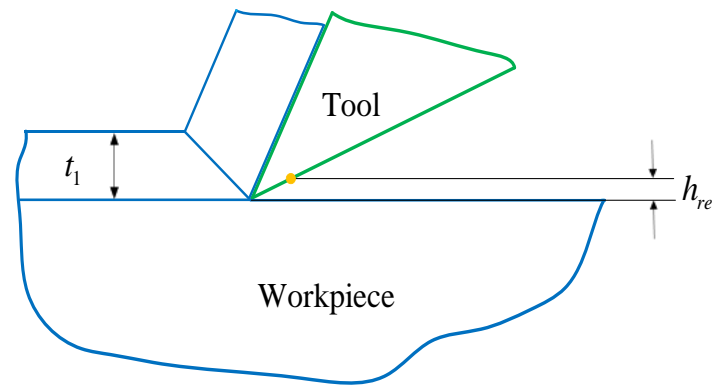


Figure 4. Tool-workpiece contact zone of sharp-edged tool.

2.5. Machining Time Model

When cutting a straight line, the cutting time can be expressed by removed the workpiece length and feed rate, $t_l = l/v_f$. The rough milling time t_{cr} can be expressed as

$$t_{cr} = \frac{l_w^r}{v_f^r} = \frac{l_w^r}{n^r z f_z^r} \tag{12}$$

The finish milling time t_{cf} can be expressed as

$$t_{cf} = \frac{l_w^f}{v_f^f} = \frac{l_w^f}{n^f z f_z^f} \tag{13}$$

where l_w^r and l_w^f are the length of the workpiece to be machined in rough and finish milling, respectively, v_f^r and v_f^f are the feed rate in rough and finish milling, respectively. n^r and n^f are the spindle speed in rough and finish machining, respectively. z is the number of tool teeth, f_z^r and f_z^f are the feed per tooth in rough and finish milling, respectively.

However, when the cutting tool passes through a corner, the feed rate is variable. Acceleration and deceleration are continuous changes in the CNC system, and the S-type acceleration and deceleration control method is widely used. The S-type acceleration and deceleration method is shown in Figure 5. The length of the line to be interpolated is L , the maximum jerk and reduced acceleration are equal to J_m , the maximum acceleration and maximum deceleration are equal to a_m , and the maximum operating speed of the machine tool is v_m . According to the acceleration change, it can be divided into seven stages: jerk, uniform acceleration, decelerated acceleration, uniform velocity, accelerated deceleration, uniform deceleration, and decelerated deceleration. The operation time of each stage is recorded as $t_1, t_2, t_3, t_4, t_5, t_6,$ and t_7 . The feed rate calculation formula is shown in Equation (14). According to the above piecewise function, the machining time of each stage can be determined from t_1 to t_7 . At the corner, the change of feed rate is shown in Figure 6.

$$v_f(\tau) = \begin{cases} v_{f1} + 0.5J_m\tau_1^2 & 0 \leq t < t_1 (\tau_1 = t) \\ v_{f2} + a_1\tau_2 & t_1 \leq t < t_2 (\tau_2 = t - t_1) & v_{f2} = v_{f1} + 0.5J_mt_1^2 \\ v_{f3} + a_1\tau_3 - 0.5J_m\tau_3^2 & t_2 \leq t < t_3 (\tau_3 = t - t_2) & v_{f3} = v_{f2} + a_1t_2 \\ v_{f4} & t_3 \leq t < t_4 (\tau_4 = t - t_3) & v_{f4} = v_{f3} + a_1t_3 - 0.5J_mt_3^2 \\ v_{f5} - 0.5J_m\tau_5^2 & t_4 \leq t < t_5 (\tau_5 = t - t_4) & v_{f5} = v_{f4} \\ v_{f6} - a_2\tau_6 & t_5 \leq t < t_6 (\tau_6 = t - t_5) & v_{f6} = v_{f5} - 0.5J_mt_5^2 \\ v_{f7} - a_2\tau_7 + 0.5J_m\tau_7^2 & t_6 \leq t < t_7 (\tau_7 = t - t_6) & v_{f7} = v_{f6} - a_2t_6 \end{cases} \tag{14}$$

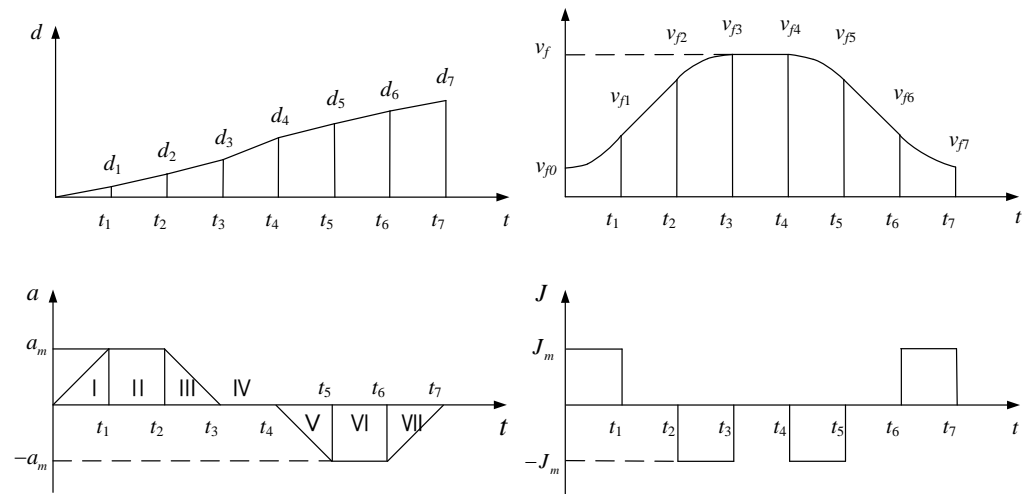


Figure 5. Velocity, accelerate, jerk and machining time in S-curve Acc/Dec process.

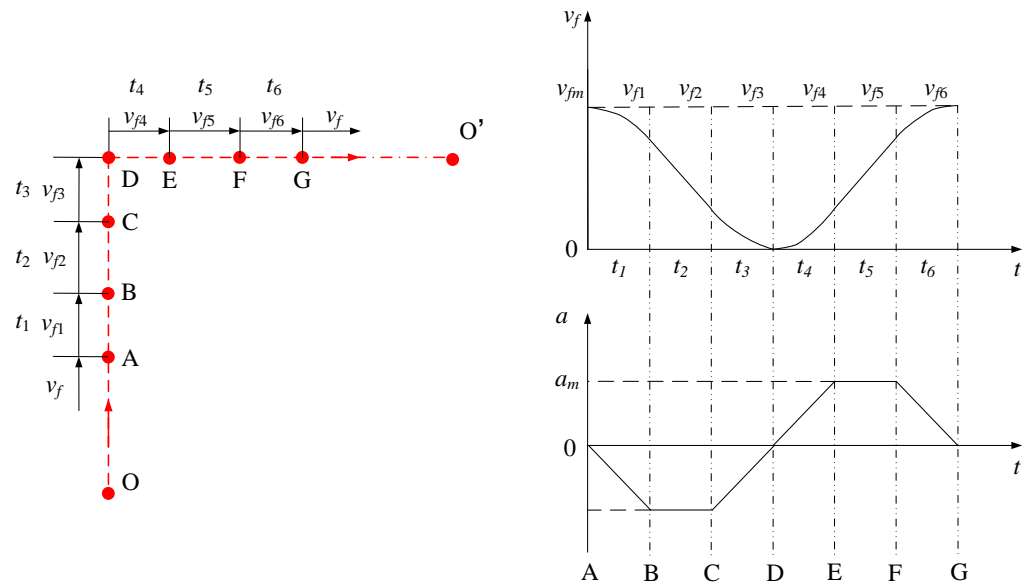


Figure 6. Schematic diagram of feed rate at corner.

Energy consumption is the integration of power in time. The model of cutting energy consumption can be calculated as Equation (15).

$$E = \int_{t_{start}}^{t_{finish}} P_c dt = \int_{t_{start}}^{t_{finish}} (K_1 a_p a_e v_f + K_2 n a_e a_p + K_3 n a_e) dt_c \tag{15}$$

3. Experimental Setup

The TC-500R machine tool (Shenyang Machine Tool Co., LTD, Shenyang, China) is used in experiment, and the fixed power is 386 W. The FLUKE Norma 5000 high-precision power analyzer (FLUKE, Everett, WA, USA) is used to measure and record the energy demand during the machining process. The FLUKE Norma 5000 high-precision power analyzer is shown in Figure 7. The accuracy of practical measurement of power depends on the measuring equipment. The accuracy of the Fluke Norma 5000 is within 0.2%. The accuracy of the AC current clamp i200 is $\pm (1\% + 0.5 \text{ A})$.

The PTHK AlTiCrN cutting tool is adopted, and the tool type is H650 $\Phi 12.0 \times 12.0 \times 30 \times 75 \times 12 \text{ DX-2F}$. The corresponding tool parameters used in the tests are as follows in Table 1. The workpiece material is Al 6061. The workpiece size is 80 mm \times 50 mm \times 200 mm. The

corresponding material properties are in Table 2. Cutting tool and workpiece are shown in Figure 8. Field map of experiment is shown in Figure 9.



Figure 7. FLUKE Norma 5000 high-precision power analyzer.

Table 1. Tool parameters.

Type of Cutter	Particle Size	Hardness	Coating	Helix Angle	Number of Edges	Material
End milling cutter	0.6 μ m	$\leq 65^\circ$	AlTiCrN	35 $^\circ$	2	Tungsten steel

Table 2. Mechanical properties of Al 6061.

Material	Yield Strength (MPa)	Ultimate Strength (MPa)	Elongation (%)	Vickers Hardness (HV)	Density (gr/cm ³)
Al 6061	286	318	5.44	106	2.7

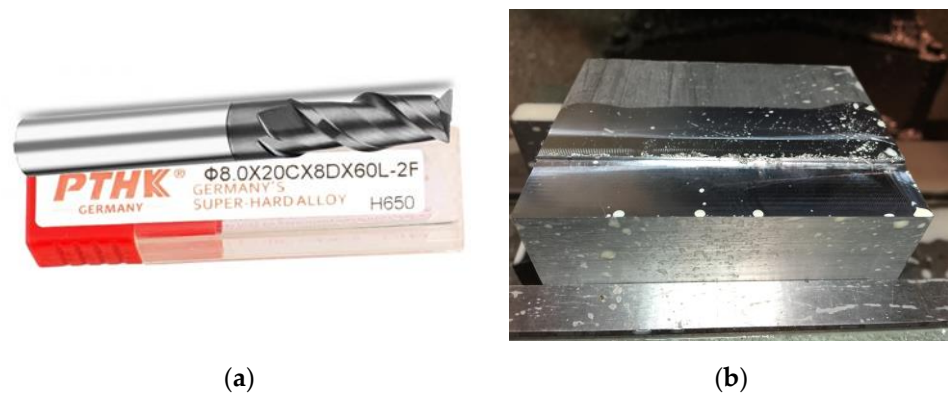


Figure 8. Cutting tool and workpiece (a) PTHK H650 cutting tool; (b) Al 6061 material workpiece.

Ten groups of experiments are designed by single factor test to verify the accuracy of the model. The spindle speed and feed rate are fixed at 400 rpm and 300 mm/min. The first five groups are used to change the cutting width, and the last five groups are used to change the cutting depth. The selection of cutting parameters is based on the research of Seçgin and Sogut [28]. The cutting parameters used in experiment are shown in Table 3.

The comparison between the measured power and the predicted power is shown in Table 4. Based on the above analysis, Equation (16) is used to calculate the error.

$$AE = 1 - \frac{|E_{mea} - E_{cal}|}{E_{mea}} \quad (16)$$

where E_{cal} is the predicted value of energy consumption, which is calculated by the energy consumption model, E_{mea} is the measured value of energy consumption, which is obtained by experiment, and AE is the prediction error.



Figure 9. Field map of experimental.

Table 3. Cutting parameters used in validation experiment.

Experiment Number	a_e (mm)	a_p (mm)	E_{cal} (J)	E_{mea} (J)	Prediction Error (%)
1	5	5	5896	6397	8.50
2	5.2	5	6132	5940	3.13
3	5.4	5	6368	6949	9.12
4	5.6	5	6603	6995	5.94
5	5.8	5	6840	6863	0.34
6	5	5	5896	6397	8.50
7	5	5.5	6486	6971	7.48
8	5	6	7075	8319	17.58
9	5	6.5	7665	8443	10.15
10	5	7	8254	8641	4.69

Table 4. Cutting parameters used in orthogonal experiment.

Experiment Number	n (rpm)	v_f (mm/min)	a_p (mm)	a_e (mm)	P_c (W)	E (J)
1	2500	200	2	0.3	7.05	530.16
2	2500	300	4	0.6	15.51	775.50
3	2500	400	6	0.9	39.36	1472.06
4	3000	200	4	0.9	21.56	1621.31
5	3000	300	6	0.3	14.41	720.50
6	3000	400	2	0.6	14.62	546.79
7	3500	200	6	0.6	20.26	1523.55
8	3500	300	2	0.9	17.77	888.5
9	3500	400	4	0.3	14.55	544.17

Figure 10 shows the accuracy of the predicted and measured cutting energy. It is found that both the predicted value and the measured value increase with cutting parameters, and the trend is consistent. It can be seen from Figure 10a that, as the cutting width increases from 5 mm to 5.8 mm, the cutting energy consumption increases slowly. It can be seen from Figure 10b that, as the cutting depth increases from 5 mm to 7 mm, the cutting energy consumption gradually increases and shows a linear growth trend. With the increase in cutting depth and cutting width, the material removal volume, tool-chip contact length, and tool-workpiece contact length increase, leading to the increase of the cutting energy consumption. The predicted cutting energy consumptions underestimate

the measured ones. This is because the model ignores the chip kinetic energy, surface energy, and elastic deformation energy. When the cutting width increases from 5 mm to 5.8 mm, the general trend of cutting energy consumption is slowly increasing, but the trend between the two values is not necessarily increasing. This may be due to the cutting width selection range being too narrow. The measured cutting power is a value that fluctuates with time. The small increment of cutting width leads to the small increment of cutting power. The measured value of cutting energy consumption shows a downward trend due to the unobvious power growth, measurement error and power fluctuation.

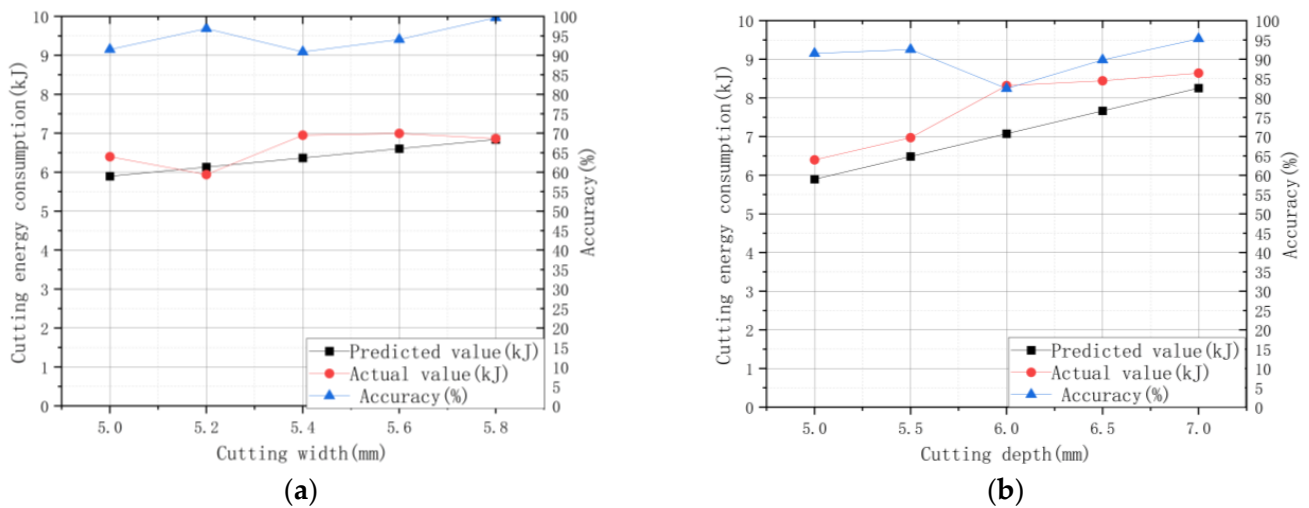


Figure 10. Comparison of calculated and measured values of cutting energy: (a) Cutting width; (b) Cutting depth.

The error between the measured value of cutting energy consumption and the predicted value of cutting energy consumption indicates the effectiveness of the developed model. The maximum error is 17.58%, respectively, and the average error is 6.64%. The prediction accuracy of the cutting power model is more than 82%. The model established in this paper can better predict the cutting energy consumption in the machining process of a three-axis machine tool.

4. Analysis of the Influence of Cutting Parameters on Cutting Energy Consumption

Once the cutting system is determined, the cutting parameters become the main factor affecting the cutting energy consumption. The cutting parameters mainly affect the cutting power and energy consumption by affecting the plastic deformation power of workpiece and the friction power at the contact interface of cutting tool and workpiece.

The influence of cutting parameters on cutting energy consumption is analyzed as follows:

According to Equation (11), plastic deformation energy is related to cutting width, cutting depth and feed rate. The friction energy on rake face is related to spindle speed, cutting width and cutting depth, and the flank face friction energy is related to spindle speed and cutting width.

The cutting width has a great influence on the cutting power. As the cutting width increases, the material removal volume increases. Therefore, the plastic deformation power increases. At the same time, with the increase of cutting width, the increase in tool-workpiece contacts zone leads to an increase in the friction power of the rake face and flank face.

Similarly, the material removal volume increases with the cutting width. Therefore, the plastic deformation power increases. Although the cutting depth is not included in the calculation of the friction power of the flank face, the proportion of the friction power of the flank face is very small for sharp-edge tools. Therefore, the plastic deformation power

and the friction power or rake face increase with the increase in the cutting depth, and the cutting depth has a great influence on the cutting power.

The change of feed rate only affects the plastic deformation energy in the cutting energy, and does not have any effect on the friction energy. The plastic deformation energy increases with feed rate. The change of spindle speed only affects the friction energy, and does not have any effect on the plastic deformation energy. The consumed friction energy increases with the increase in spindle speed.

By comparing the proportional coefficients of the cutting parameters, it is found that, when cutting width is greater than cutting depth, cutting depth has the greatest impact on the cutting power, followed by cutting width, the feed rate, and the spindle speed. When cutting depth is greater than cutting width, cutting width has the greatest impact on the cutting power, followed by the cutting width, then the feed rate, and finally the spindle speed.

To study the influence of cutting parameters on cutting energy consumption, the Taguchi experimental design method is used to analyze cutting energy consumption. The spindle speed, feed rate, cutting depth and cutting width are selected as the experimental factors, and the L9 orthogonal table of 9 groups of experiments with 4 factors and 3 levels is used for experiments. The experimental results are shown in Table 4.

The extremum difference analysis method can be used to determine the primary and secondary relationship between cutting parameters and cutting power and cutting energy consumption. The greater the extremum difference value, the greater the influence of the corresponding factors on the cutting power.

According to the results of the orthogonal test, the extremum difference statistics are carried out, and the results are shown in Tables 5 and 6. As shown in Figures 11 and 12, the main effect diagram of cutting power and cutting energy are analyzed by Minitab, respectively. The slope of the main effect diagram can reflect the influence of each parameter on the cutting power and energy. The horizontal axis in the figure is the controllable level value of each factor.

Table 5. Range statistics of cutting power.

Experiment Number	n (rpm)	v_f (mm/min)	a_p (mm)	a_e (mm)
1	20.65	16.29	13.15	12.01
2	16.87	15.90	17.21	16.80
3	17.53	22.85	24.68	26.24
Calculation rank	3.78	6.95	11.54	14.23
Rank	$a_e > a_p > v_f > n$			

Table 6. Range statistics of cutting energy consumption.

Experiment Number	n (rpm)	v_f (mm/min)	a_p (mm)	a_e (mm)
1	925.9	1225.0	655.1	598.3
2	962.9	794.8	980.3	948.6
3	985.4	854.3	1238.7	1327.3
Calculation rank	59.5	430.2	583.6	729.0
Rank	$a_e > a_p > v_f > n$			

According to main effect diagram, the cutting width is the main influencing factor, followed by cutting depth, feed rate, and spindle speed. The cutting power increases with cutting width and cutting depth. The reason is that the cutting zone increases and the friction power increases with cutting width and cutting depth. At the same time, cutting power increases with the plastic deformation power. When $n < 3000$ r/min, cutting power

decreases with the increase in spindle speed. When $n > 3000$ r/min, the cutting power increases slowly with the spindle rate continuing to increase. When $v_f < 300$ mm/min, the unit pressure of the rake face is small with the increase in the feed rate, and the friction coefficient is constant. Therefore, the cutting power changes slightly. When $v_f > 300$ mm/min, the cutting power increases with the feed rate continuing to increase. As the feed rate increases, the cutting zone increases, and the friction energy increases. Therefore, reducing the cutting power of the machine tool by changing cutting width or the cutting depth is more effective than changing feed rate and spindle speed.

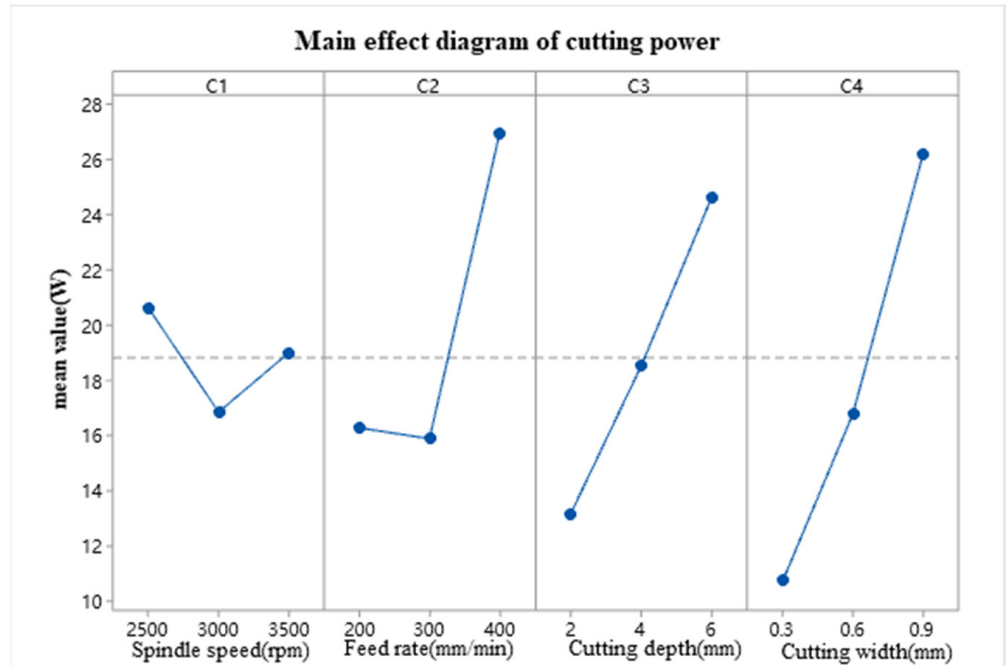


Figure 11. Main effects plot of cutting power.

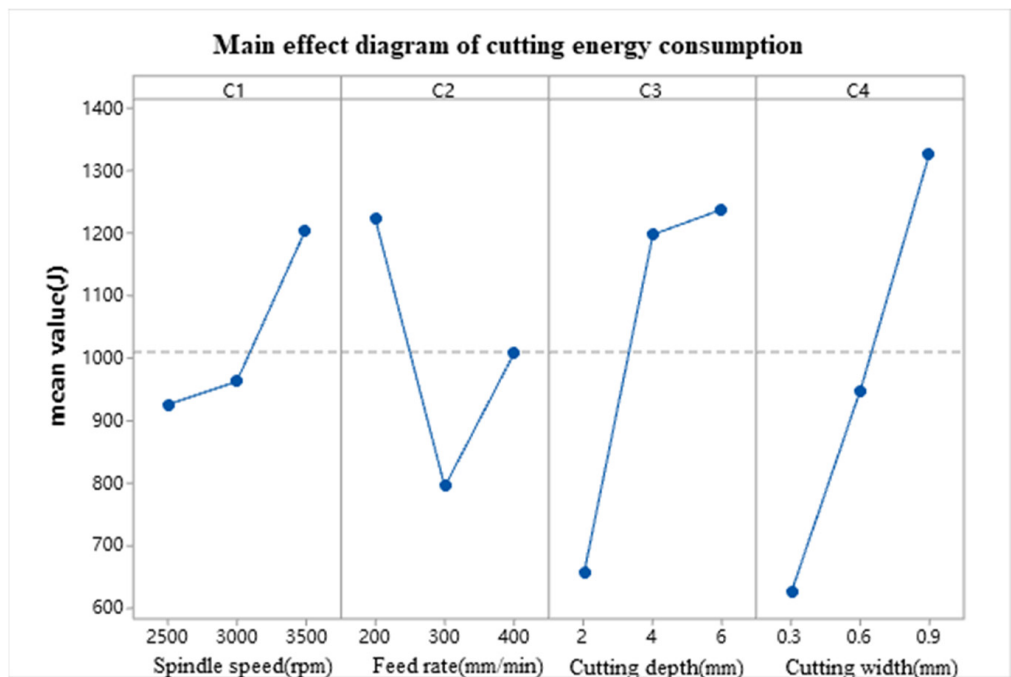


Figure 12. Main effects plot of cutting energy.

The cutting power values of the optimal cutting parameters and other cutting parameters measured experimentally are compared. Similarly, to obtain the parameter value with the minimum cutting energy consumption during machine tool processing, small spindle speed, cutting depth and cutting width, moderate or large feed speed should be selected. As shown in Figures 13 and 14 it is found that the optimal combination of cutting parameters $n = 3000$, $v_f = 300$, $a_p = 2$, and $a_e = 0.3$ is the smallest combination out of 81 groups of cutting power values.

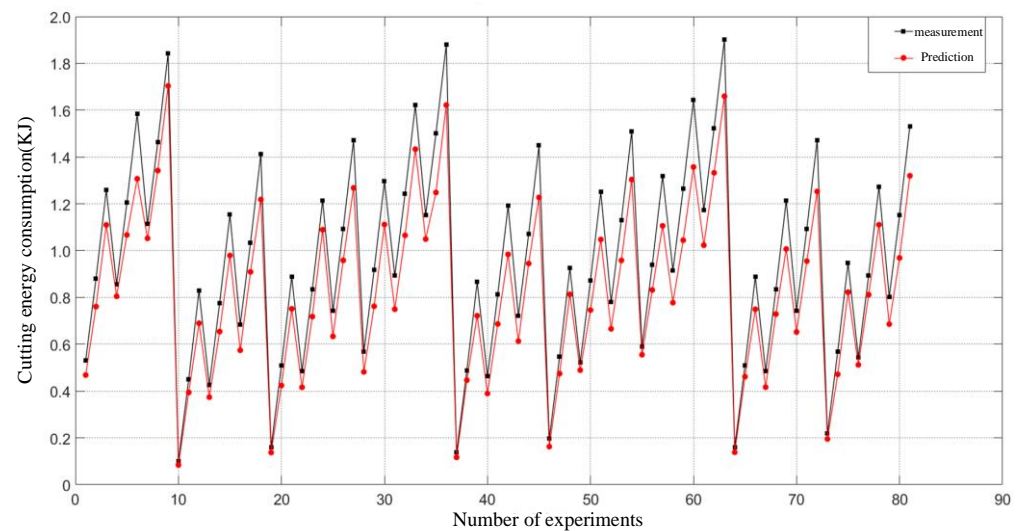


Figure 13. Measured and predicted values of cutting energy.

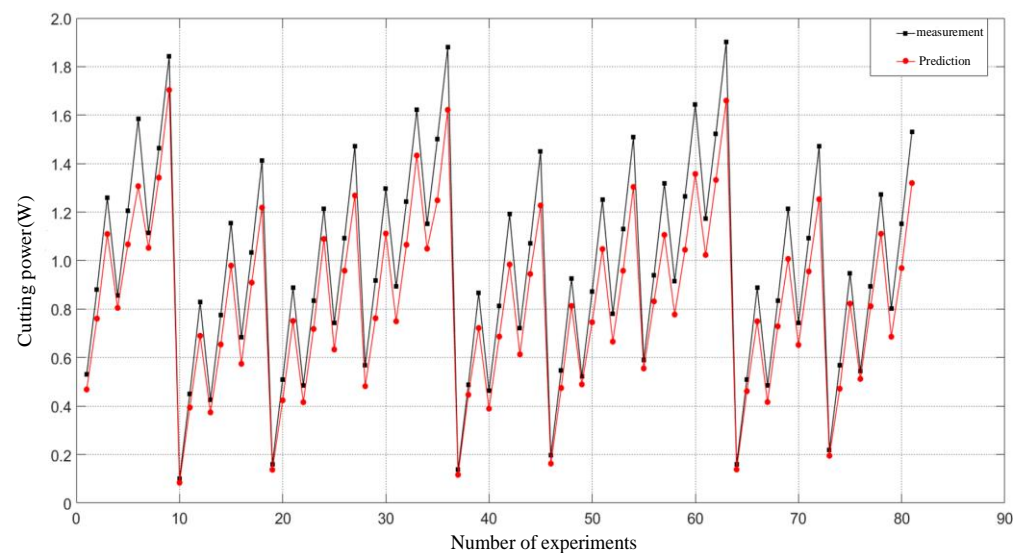


Figure 14. Measured and predicted values of cutting power.

5. Conclusions

In this paper, a cutting energy consumption modelling method considering material shear deformation and tool–workpiece friction characteristics is proposed for the influence of chips on cutting energy consumption. The cutting energy consumption model is composed of a machining time model and a cutting power model. The influence of chip and tool edge geometry on cutting power is considered from the perspective of chip forming, then the cutting power model is improved. The S-type acceleration and deceleration process is used to improve the machining time model. The prediction accuracy of the cutting energy consumption model is verified to be above 82% by milling steps. The

influence of cutting parameters on the energy consumption of the machine tool is analyzed by the Taguchi experiment. It is found that the cutting width is the main influencing factor, followed by cutting depth, feed speed, and spindle speed. In this paper, the established model method can be used to predict the cutting energy consumption of each machine tool. The model can be used to optimize the cutting parameters to reduce energy consumption. Recommendations are provided for factories to reduce cutting energy consumption in machining. The chip kinetic energy gradually increases with the cutting speed. When high-speed cutting is performed, the chip kinetic energy cannot be ignored. To solve this problem, future research work will study the modelling method of chip kinetic energy and cutting energy consumption.

Author Contributions: Idea proposal, Y.M. and X.L.; Model establishment, all authors; Experimental design, S.D. and Y.W.; Experimental verification, X.S. and S.D.; Result analysis, Y.M. and X.S.; writing—original draft preparation X.S.; writing—review and editing, all authors; All authors have read and agreed to the published version of the manuscript.

Funding: This work is supported by the National Natural Science Foundation of China (Grant No: 51720105009).

Institutional Review Board Statement: Not applicable.

Informed Consent Statement: Not applicable.

Data Availability Statement: Not applicable.

Conflicts of Interest: The authors declare no conflict of interest.

References

1. Newman, S.T.; Nassehi, A.; Imani-Asrai, R.; Dhokia, V. Energy efficient process planning for CNC machining. *CIRP J. Manuf. Sci. Technol.* **2012**, *5*, 127–136. [\[CrossRef\]](#)
2. Bi, Z. Revisiting system paradigms from the viewpoint of manufacturing sustainability. *Sustainability* **2011**, *3*, 1323–1340. [\[CrossRef\]](#)
3. Gutowski, T.; Dahmus, J.; Thiriez, A. Electrical energy requirements for manufacturing processes. In Proceedings of the 13th CIRP International Conference on Life Cycle Engineering, Leuven, Belgium, 31 May–2 June 2006; Volume 31, pp. 623–638.
4. Zhou, L.; Li, F.; Zhao, F.; Li, J.; Sutherland, J.W. Characterizing the effect of process variables on energy consumption in end milling. *Int. J. Adv. Manuf. Technol.* **2018**, *101*, 2837–2848. [\[CrossRef\]](#)
5. Balogun, V.A.; Gu, H.; Mativenga, P.T. Improving the integrity of specific cutting energy coefficients for energy demand modelling. *Proc. Inst. Mech. Eng. Part B J. Eng. Manuf.* **2014**, *229*, 2109–2117. [\[CrossRef\]](#)
6. Rodriguez-Alabanda, O.; Bonilla, M.T.; Guerrero-Vaca, G.; Romero, P.E. Selection of parameters and strategies to reduce energy consumption and improve surface quality in EN-AW 7075 molds machining. *Metals* **2018**, *8*, 688. [\[CrossRef\]](#)
7. Rodrigues, A.R.; Coelho, R.T. Influence of the tool edge geometry on specific cutting energy at high-speed cutting. *J. Braz. Soc. Mech. Sci. Eng.* **2007**, *29*, 279–283. [\[CrossRef\]](#)
8. Liu, Z.Y.; Guo, Y.B.; Sealy, M.P.; Liu, Z.Q. Energy consumption and process sustainability of hard milling with tool wear progression. *J. Mater. Process. Technol.* **2016**, *229*, 305–312. [\[CrossRef\]](#)
9. Liu, Z.Y.; Sealy, M.P.; Li, W.; Zhang, D.; Fang, X.Y.; Guo, Y.B.; Liu, Z.Q. Energy consumption characteristics in finish hard milling. *J. Manuf. Process.* **2018**, *35*, 500–507. [\[CrossRef\]](#)
10. Zhang, T.; Liu, Z.Y.; Sun, X.; Xu, J.; Dong, L.; Zhu, G. Investigation on specific milling energy and energy efficiency in high-speed milling based on energy flow theory. *Energy* **2019**, *192*, 116596. [\[CrossRef\]](#)
11. Nur, R.; Yusof, N.M.; Sudin, I.; Nor, F.M.; Kurniawan, D. Determination of Energy Consumption during Turning of Hardened Stainless Steel Using Resultant Cutting Force. *Metals* **2021**, *11*, 565. [\[CrossRef\]](#)
12. Shao, H.; Wang, H.L.; Zhao, X.M. A cutting power model for tool wear monitoring in milling. *Int. J. Mach. Tools Manuf.* **2004**, *44*, 1503–1509. [\[CrossRef\]](#)
13. Li, B.; Tian, X.; Zhang, M. Modeling and multi-objective optimization method of machine tool energy consumption considering tool wear. *Int. J. Precis. Eng. Manuf.-Green Technol.* **2022**, *71*, 1133–1142. [\[CrossRef\]](#)
14. Shi, K.N.; Zhang, D.H.; Liu, N.; Wang, S.B.; Ren, J.X.; Wang, S.L. A novel energy consumption model for milling process considering tool wear progression. *J. Clean. Prod.* **2018**, *184*, 152–159. [\[CrossRef\]](#)
15. Jiang, B.; Li, H.; Fan, L.; Zhao, P. A Model for Energy Consumption of Main Cutting Force of High Energy Efficiency Milling Cutter under Vibration. *Appl. Sci.* **2022**, *12*, 1531. [\[CrossRef\]](#)
16. Awan, M.R.; Rojas, H.A.G.; Hameed, S.; Riaz, F.; Hamid, S.; Hussain, A. Machine Learning-Based Prediction of Specific Energy Consumption for Cut-Off Grinding. *Sensors* **2022**, *22*, 7152. [\[CrossRef\]](#)

17. Brillinger, M.; Wuwer, M.; Hadi, M.A.; Haas, F. Energy prediction for CNC machining with machine learning. *CIRP J. Manuf. Sci. Technol.* **2021**, *35*, 715–723. [[CrossRef](#)]
18. Pawanr, S.; Garg, G.K.; Routroy, S. Modelling of Variable Energy Consumption for CNC Machine Tools. *Procedia CIRP* **2021**, *98*, 247–251. [[CrossRef](#)]
19. Yu, S.; Zhao, G.; Li, C.; Xu, S.; Zheng, Z. Prediction models for energy consumption and surface quality in stainless steel milling. *Int. J. Adv. Manuf. Technol.* **2021**, *117*, 3777–3792. [[CrossRef](#)]
20. Pawanr, S.; Garg, G.K.; Routroy, S. Development of a Transient Energy Prediction Model for Machine Tools. *Procedia CIRP* **2021**, *98*, 678–683. [[CrossRef](#)]
21. Zhao, G.; Su, Y.; Zheng, G.; Zhao, Y.; Li, C. Tool tip cutting specific energy prediction model and the influence of machining parameters and tool wear in milling. *Proc. Inst. Mech. Eng. Part B J. Eng. Manuf.* **2020**, *234*, 1346–1354. [[CrossRef](#)]
22. Ma, J.; Ge, X.; Chang, S.I.; Lei, S. Assessment of cutting energy consumption and energy efficiency in machining of 4140 steel. *Int. J. Adv. Manuf. Technol.* **2014**, *74*, 1701–1708. [[CrossRef](#)]
23. Abele, E.; Braun, S.; Schraml, P. Holistic Simulation Environment for Energy Consumption Prediction of Machine Tools. *Procedia CIRP* **2015**, *29*, 251–256. [[CrossRef](#)]
24. Pawar, S.S.; Bera, T.C.; Sangwan, K.S. Energy consumption modelling in milling of variable curved geometry. *Int. J. Adv. Manuf. Technol.* **2022**, *120*, 1967–1987. [[CrossRef](#)]
25. Zhou, L.; Li, F.; Wang, L.; Wang, Y.; Wang, G. A new energy consumption model suitable for processing multiple materials in end milling. *Int. J. Adv. Manuf. Technol.* **2021**, *115*, 2521–2531. [[CrossRef](#)]
26. Ammarullah, M.I.; Santoso, G.; Sugiharto, S.; Supriyono, T.; Wibowo, D.B.; Kurdi, O.; Tauviqirrahman, M.; Jamari, J. Minimizing Risk of Failure from Ceramic-on-Ceramic Total Hip Prosthesis by Selecting Ceramic Materials Based on Tresca Stress. *Sustainability* **2022**, *14*, 13413. [[CrossRef](#)]
27. Ammarullah, M.I.; Santoso, G.; Sugiharto, S.; Supriyono, T.; Kurdi, O.; Tauviqirrahman, M.; Wonarni, T.I.; Jamari, J. Tresca stress study of CoCrMo-on-CoCrMo bearings based on body mass index using 2D computational model. *J. Tribol.* **2022**, *33*, 31–38.
28. Seçgin, Ö.; Sogut, M.Z. Surface roughness optimization in milling operation for aluminum alloy (Al 6061-T6) in aviation manufacturing elements. *Aircr. Eng. Aerosp. Technol.* **2021**, *93*, 1367–1374. [[CrossRef](#)]

Disclaimer/Publisher’s Note: The statements, opinions and data contained in all publications are solely those of the individual author(s) and contributor(s) and not of MDPI and/or the editor(s). MDPI and/or the editor(s) disclaim responsibility for any injury to people or property resulting from any ideas, methods, instructions or products referred to in the content.